



Research paper

Selective recognition of Zn(II) ions in live cells based on chelation enhanced near-infrared fluorescent probe

Yibin Zhang^a, Binfang Yuan^{a,*}, Dongge Ma^{b,*}

^a Chongqing Key Laboratory of Inorganic Special Functional Materials, College of Chemistry and Chemical Engineering, Yangtze Normal University, Fuling, Chongqing 408100, PR China

^b School of Science, Beijing Technology and Business University, Beijing 100048, PR China

ARTICLE INFO

Keywords:

Near-infrared fluorescence
Dicyanoisophorone derivative
Zn(II)
Cellular imaging

ABSTRACT

A near-infrared fluorescent (NIR) probe NR-Zn, which consists of a dicyanoisophorone derivative and an Zn(II) ion recognitive dipicolylamine moiety, was synthesized and applied to detect Zn(II) ions concentration change in living cell. This NR-Zn probe exhibits a strong turn-on fluorescence response toward Zn(II) ions when excited at 545 nm and has other advantages, such as rapid response (< 20 s), large Stokes shift (131 nm), low cytotoxicity and good photostability. Moreover, it has been successfully applied to monitor Zn(II) ions in Hela cells.

1. Introduction

Zn(II) ion is an essential transition metal nutrient for life, which ranks the second abundant metal element after iron in the human body. It is extensively involved in a broad range of biological processes such as enzyme regulation [1], DNA synthesis [2], neurotransmission [3], apoptosis regulation [4], cellular transport [5], metabolism [6], etc. Abnormal levels of Zn(II) ions can lead to many diseases, for examples, Alzheimer's disease, epilepsy [7], ischemic stroke [8] and prostate cancer [9]. Besides, zinc is released by a range of industrial and sewage runoff, resulting in abnormal high Zn(II) ions concentration in air, water or soil environment, which can cause harmful effects for human-being. Therefore, it is necessary to precisely detect Zn(II) ions concentration for the understanding of its function in biological, physiological and pathological processes. On the other hand, the accurate detection of Zn(II) ion concentration in the natural environment will also benefit environmental protection.

In recent years, *in-vivo* and *in-vitro* fluorescent imaging techniques based on organic small molecule probes have been widely applied in living systems to unveil the cellular functions of metal ions due to its high sensitivity, spatial resolution, and easy high temporal modulation in biological samples [10–18]. Although a good deal of Zn(II) ions fluorescent probes have been reported and applied for imaging in living cells, many of these exhibited shortcomings such as long response time (typically > 20 min), narrow Stokes shift (< 60 nm), severe photo-damage to biological samples and auto-fluorescence interference because of their short-wavelength emission in < 600 nm window

[19–27]. In order to overcome these limitations, near-infrared fluorescent probes are developed to meet the need including their minimal background interference, improved tissue depth penetration and high image sensitivities and spatial resolution for *in-vivo* imaging application. However, only a few near-infrared fluorescent probes of Zn(II) ions were reported and it still remains an urgent demand to develop novel near-infrared fluorescent probes to detect Zinc (II) ion concentration *in-vivo* [28–36].

Herein, we present a novel near-infrared fluorescent probe NR-Zn for highly sensitive detection of Zn(II) ion concentration by employing dicyanoisophorone group as a recognition moiety based on the chelation reaction, as shown in Scheme 1. The synthesis route of probe NR-Zn is discussed in detail, and this probe displays very weak and imperceptible fluorescence emission in the absence of Zn(II) ions. However, a significantly enhanced near-infrared fluorescence emission at 660 nm is switched on upon the addition of Zn(II) ions, which release the hydroxyl group as a strong electron donor via the chelation of Zn(II)-binding ligand. Moreover, experiments results also demonstrate that this probe has low cytotoxicity, high selectivity for Zn(II) ions and excellent photo-stability. Finally, it exhibited its potential for *in-vivo* and clinical applications by the dynamic monitoring of the fluctuation of Zn(II) ions concentration in Hela cells.

* Corresponding authors.

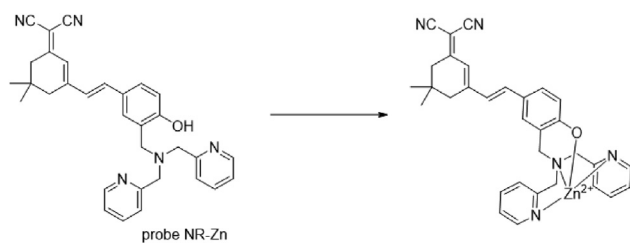
E-mail addresses: zhangyibin@yznu.edu.cn (Y. Zhang), 6781022@163.com (B. Yuan), madongge@btbu.edu.cn (D. Ma).

<https://doi.org/10.1016/j.ica.2020.119640>

Received 16 February 2020; Received in revised form 30 March 2020; Accepted 30 March 2020

Available online 31 March 2020

0020-1693/ © 2020 Elsevier B.V. All rights reserved.



Scheme 1. The structure of the probe NR-Zn and its interaction mode with Zn(II) ion.

2. Experimental section

2.1. Instrumentation

Varian Unity Inova 500 MHz Spectrometer is used for ^1H NMR and ^{13}C NMR spectra. Perkin Elmer Lambda 35 UV/VIS spectrometer is used for absorption spectra and Horiba FluoroMax-4 Spectrofluorometer is used for fluorescence spectroscopy. Analysis Olympus IX 81 confocal laser scanning microscope is used for cell imaging.

2.2. Reagents

All reagents were bought from Sigma-Aldrich without further purification, and the reactions were carried out under nitrogen condition.

2.3. Imaging

The procedures of Probe NR-Zn applying in the detection of Zn(II) concentration in Hela cells are similar as we previously reported [37].

2.4. Synthesis

4-Hydroxy benzaldehyde (610 mg, 5 mmol), bis(pyridin-2-ylmethyl)amine (1 g, 5 mmol) and paraformaldehyde (290 mg, 10 mmol) were added together and then stirred at $50\text{ }^\circ\text{C}$ overnight under N_2 . The resulting mixture was evaporated and purified by flash column chromatography to get compound 1 as a yellow liquid. ^1H NMR (400 MHz, CDCl_3) δ 9.78 (s, 1H), 8.54 (s, 2H), 7.84–7.49 (m, 4H), 7.36–7.09 (m, 4H), 7.09–6.90 (m, 1H), 3.85 (s, 4H), 3.77 (s, 2H). ^{13}C NMR (101 MHz, CDCl_3) δ 190.77, 164.13, 158.06, 148.88, 137.10, 132.41, 132.36, 128.47, 123.91, 123.23, 122.50, 117.56, 59.02, 56.66. HRMS for $[\text{C}_{20}\text{H}_{19}\text{N}_3\text{O}_2 + \text{H}^+]$: 334.1477; found: $[\text{M} + \text{H}]^+$ 334.1549.

3-((bis(pyridin-2-ylmethyl)amino)methyl)-4-hydroxybenzaldehyde (333 mg, 1 mmol), 2-(3,3,5-trimethylcyclohexylidene)malononitrile (188 mg, 1 mmol), piperidine (1 drop) were added in 10 mL ethanol. This mixture was stirred at $60\text{ }^\circ\text{C}$ for 8 h under N_2 , then the mixture was evaporated under reduced pressure, and extracted by DCM for three times, the organic layers were combined and was purified by flash column chromatography to get probe NR-Zn as a yellow solid. ^1H NMR (400 MHz, CDCl_3) δ 8.55 (d, $J = 4.9$, 2H), 7.62 (t, $J = 7.72$ Hz), 7.40–7.21 (m, 5H), 7.16 (d, $J = 8.1$ Hz, 2H), 7.02–6.87 (m, 2H), 6.87–6.78 (m, 1H), 6.76 (s, 1H), 3.84 (s, 2H), 3.75 (s, 2H), 2.56 (s, 3H), 2.43 (s, 2H), 1.04 (s, 6H). ^{13}C NMR (101 MHz, CDCl_3) δ 169.37, 160.08, 158.19, 154.78, 148.93, 137.58, 130.16, 129.32, 126.23, 123.97, 117.78, 114.04, 113.25, 76.94, 59.10, 57.05, 43.30, 39.54, 32.32, 28.34. HRMS for $[\text{C}_{32}\text{H}_{31}\text{N}_5\text{O} + \text{H}^+]$: 502.2529; found: $[\text{M} + \text{H}]^+$ 502.2600.

3. Results and discussion

3.1. Design and synthesis of probe NR-Zn

The detailed synthetic route for probe NR-Zn is summarized in Scheme 2. The probe NR-Zn consists of dicyanoisophosphorone, a widely used building-block for fluorescent molecule skeleton [38], and

dipicolylamine (DPA), a well known Zn(II) ions chelating ligand [39]. Dicyanoisophosphorone and compound 1 was synthesized according to the previous report, the dicyanoisophosphorone was reacted with 4-hydroxy benzaldehyde under the basic condition to get the required probe. The total yield of the two steps is 56%, the ^1H NMR, ^{13}C NMR spectrometry and high-resolution mass spectrometry (HRMS) of this probe are shown in the ESI.

3.2. UV-Vis absorption and fluorescence response of probe NR-Zn toward Zn(II) ions

After we obtained probe NR-Zn, we first assessed the UV-Vis absorption and fluorescence response of this probe toward different concentrations of Zn(II) ions. As shown in the absorption spectra of Fig. 1, The probe NR-Zn displays a maximum absorption peak at 425 nm in HEPES buffer. However, in the presence of Zn(II) ions, the absorption peak exhibited a 30 nm red shift and appeared at 455 nm with the solution color changes from colorless to pale red. At the same time, the free probe displayed a very weak fluorescence, upon addition of Zn(II) ions, a significantly enhanced emission around 660 nm was observed under 545 nm excitation, which resided in the near-infrared fluorescent region. This switch-on emission was perhaps attributed to the ICT effect (intramolecular charge transfer) and chelation enhanced fluorescence (CHEF) triggered by chelating Zn(II) ions to the probe. This probe exhibits a remarkable large pseudo-Stokes shift of 110 nm, which is highly beneficial to reduce the influence of scattering of excitation light and interference from background fluorescence in practical applications.

3.3. Sensing mechanism

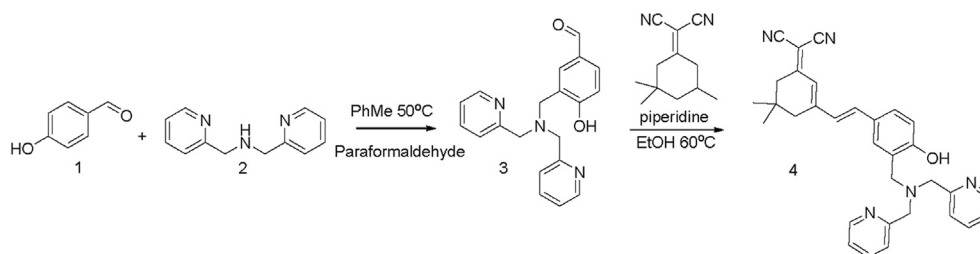
In order to investigate the sensing mechanism, pH dependency on fluorescence intensity of probe NR-Zn in the absence of Zn(II) ions was conducted at various pH values in an ethanol-buffer (3:7, v/v) solution. As shown in Fig. 2, the fluorescence emission obviously was enhanced when the probe NR-Zn was in an alkaline environment with the mixture solution color changing from faint yellow to purple. Besides, the emission performance of the probe is sensitive to pH change and it has a pKa value of 8.5 (Fig. S7). A reasonable explanation for this phenomenon is the phenoxy group was deprotonated at high pH and the transformation from phenol to phenolate induced the ICT effect between dicyanoisophosphorone (electron acceptor) and phenolate (electron donor) on the forming conjugated system. That means the structural transformation from phenol to phenolate is a critical factor for enhanced fluorescence. Thus, we considered that by binding Zn(II) ions with the probe (CHEF) to release phenolate group can also motivate the same ICT effect to increase the fluorescence of probe NR-Zn.

Next, the binding stoichiometry of probe NR-Zn with Zn(II) ions was measured by Job's plot method (Fig. 3). Through this method, different mole ratios of probe NR-Zn and Zn(II) ion were added in the ethanol-buffer (3:7, v/v) solution. It can be found that the maximum fluorescence intensity was at 0.5 mol fraction, which means the binding composition of Zn(II) ion and the probe is 1:1. Next, the binding constant value of Zn(II) ions with receptor has been determined from the emission intensity data following the modified Benesi-Hildebrand equation:

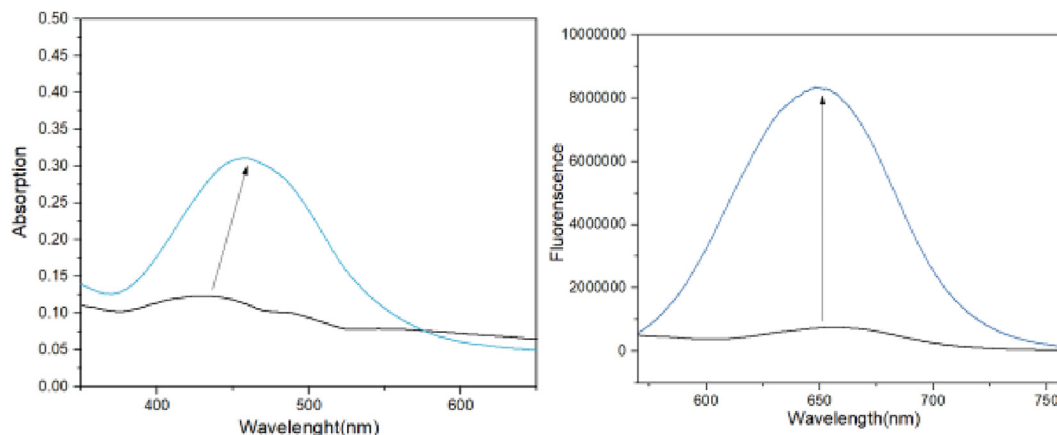
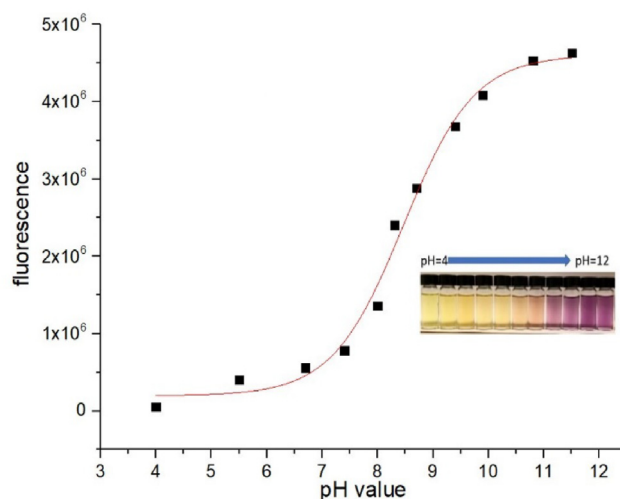
$$1/\Delta I = 1/\Delta I_{\max} + (1/Ka[C])(1/\Delta I_{\max})$$

here $\Delta I = I - I_{\min}$ and $\Delta I_{\max} = \Delta I_{\max} - I_{\min}$, where I_{\min} , I , and I_{\max} are the emission intensities of receptor considered in the absence of Zn(II) ions, at an intermediate Zn(II) ions concentration, and at a concentration of complete saturation where K is the binding constant and $[C]$ is the Zn(II) ion concentration, respectively. It can be found the plot of $1/\Delta I$ versus $1/[\text{Zn}^{2+}]$ is linear ($R = 0.9935$) and the binding constant (K_a) was 2.15×10^5 (Fig. S8).

Fluorescence quantum yields of this probe were also calculated according to literature using the equation below. Φ represents



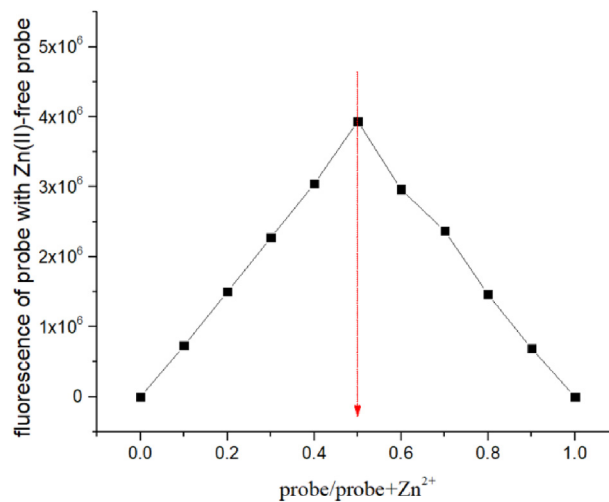
Scheme 2. The main method of synthesis of probe NR-Zn.

Fig. 1. UV-vis absorption and fluorescence spectra of 20 μM probe NR-Zn upon addition of 100 μM Zn(II) ions (in ethanol /pH 7.4 HEPES buffer = 3/7, 0.9 mL/2.7 mL).Fig. 2. Fluorescence intensity changes of 10 μM probe NR-Zn in different pH value (in ethanol /pH 7.4 HEPES buffer = 3/7, 0.9 mL/2.7 mL).

fluorescence quantum yield. I_x is integration of sample's fluorescence spectra at specific excitation wavelength. A is the absorbance at the specific excited wavelength while the absorbance at the wavelength of excitation is optimally kept between 0.02 and 0.05, n is the refractive index of solvents which were used for optical measurements, and the subscripts x and st stand for the probe and a reference compound of known fluorescence quantum yield, respectively [40].

$$\phi_x = \phi_{st} \frac{\eta_x^2 A_{st} I_x}{\eta_{st}^2 A_x I_{st}}$$

Rhodamine 6G was used as a standard to calculate quantum yield at 450 nm excitation [41]. The fluorescence quantum yield of probe increases from 0.048 to 0.21, along with the molar absorptivity changes

Fig. 3. Job's plots of the fluorescence of the probe NR-Zn with different concentrations of Zn^{2+} (fluorescence intensity was calculated by the actual fluorescence intensity of probe with Zn^{2+} remove the blank fluorescence intensity of free probe, in ethanol /pH 7.4 HEPES buffer = 3/7, 0.9 mL/2.7 mL).

from $1.52 \times 10^4 \text{ M}^{-1}\text{cm}^{-1}$ to $3.43 \times 10^4 \text{ M}^{-1}\text{cm}^{-1}$, in the absence and presence of Zn(II) ion (30% ethanol with pH buffer 7.4), respectively. This means that binding Zn(II) ions can significantly improve the intensity of the fluorescence signal of probe NR-Zn, which is critical to detect Zn(II) ions sensitively.

Next, the binding site of the probe NR-Zn towards Zn(II) ions were investigated by ^1H NMR titration experiment. As shown in Fig. 4 and Fig. S9, the free probe NR-Zn exhibited a phenoxy ($-\text{OH}$) signal at 7.62 ppm in $\text{DMSO}-d_6$. After 1.0 equiv of Zn(II) ions was added, the signal of hydroxyl proton immediately diminished, which verified the binding of Zn(II) ions with hydroxyl. Furthermore, compared with the

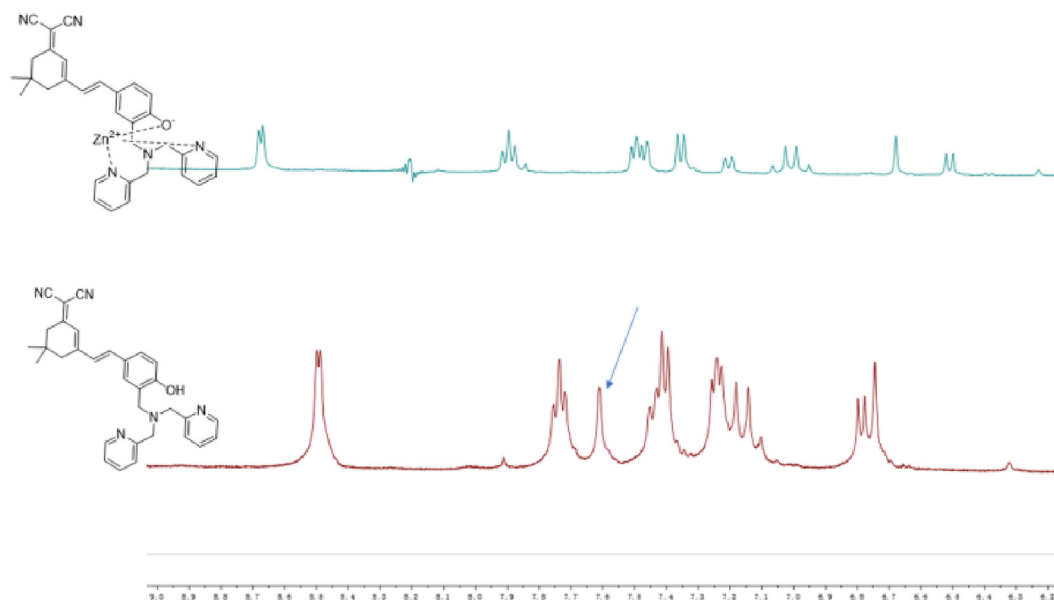


Fig. 4. Part of ^1H NMR spectrum of free probe in DMSO-d_6 and probe- Zn^{2+} in DMSO-d_6 .

free probe, the binding of Zn(II) ions induced the low-fielding of other hydrogens in the benzene ring, which means the structural transformation evoked an ICT effect and extended the whole molecule's conjugation. To further explore the structure of the complex, we used MALDI-TOF mass spectrometry to analyze the complex, when 1.0 equiv of Zn(II) ions was added to the solution of the probe, a new signal of $m/z = 564.15$ appeared accompanying with the disappearance of the signal of probe NR-Zn. 564.15 is the molecular weight of probe NR-Zn + $[\text{Zn}^{2+}]$, which reconfirms that Zn(II) ions have been chelated to the probe (Fig. 10 and Fig. S11).

3.4. Time response of probe NR-Zn toward Zn(II) ions

The response time is a very important parameter to fluorescent probes. We studied the fluorescence response time of this probe toward the change of probe for Zn(II) ions. The result was shown in Fig. 5, it shows the fluorescence intensity changes at 660 nm reached highest within less than 20 s, which was much shorter compared with other previously reported Zn(II) ions probes [28–34]. This rapid response means that it has high sensitivity to Zn(II) ions and endows it the potential for real-time monitoring of Zn(II) ions in biological systems.

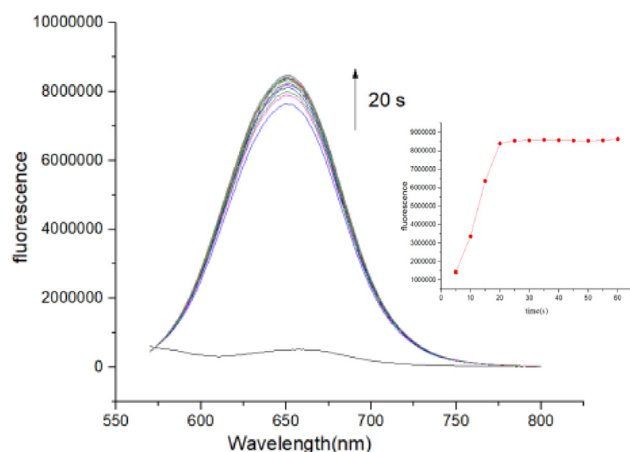


Fig. 5. Time response of 20 μM probe NR-Zn toward Zn(II) ions 20 μM . (in ethanol /pH 7.4 HEPES buffer = 3/7, 0.9 mL/2.7 mL).

3.5. Selectivity of probe NR-Zn toward Zn(II) ions

The selectivity of probe NR-Zn to Zn^{2+} over other metal ions was also evaluated, including NaCl, KCl, $\text{Ca}(\text{NO}_3)_2$, MgSO_4 , SnCl_2 , CoCl_2 , MnSO_4 , NiCl_2 , PbCl_2 , $\text{Fe}(\text{NO}_3)_2$, FeCl_3 , CuSO_4 , CdCl_2 , Cs_2CO_3 , $\text{Al}_3(\text{NO}_3)_2$, HgCl_2 . As shown in Fig. 6, there is no obvious changes upon the addition of other metal ions in the fluorescence spectrum except Cd^{2+} . Only Zn(II) ions adding to the probe-containing solution can induce about 20-fold fluorescence enhancement at 660 nm under the same conditions. Besides, the competitive experiment was conducted to estimate the specificity of probe towards Zn(II) ions, as the competition test shows, probe NR-Zn treated with 1.0 equiv. of Zn(II) ions in the presence of various competitive ions (5.0 equiv.), the fluorescence intensities of probe solution were not obviously interfered with by the co-existing metal ions. Thus, these results show that the probe NR-Zn has an excellent selective binding effect to Zn(II) ions, resulting in good selectivity for Zn(II) ions toward various other metal ions.

3.6. Linear relationship between the fluorescence response of NR-Zn and total Zn(II) ion concentration

With the optimized conditions in hand, we next investigate the linear relationship between the probe NR-Zn and Zn(II) ion concentration by titration experiment. As shown in Fig. 7, upon addition of Zn(II) ions in the range from 0–15 μM to the 10 μM probe, the fluorescence response shows a good linear relationship ($R^2 = 0.9985$) between the concentrations of Zn(II) ions and the fluorescence intensity, indicating the capability of probe NR-Zn for quantitative detection of Zn(II) ions by the fluorometric assay.

3.7. Photostability of the probe NR-Zn

The photostability is a crucial parameter to evaluate whether the probe can be used in long-time in-vivo imaging applications. Thus, the photostability of probe NR-Zn with Zn(II) ions was measured by record fluorescent intensity of probe NR-Zn under continuous 545 nm excitation. The fluorescence intensity of 10 μM probe with 20 μM Zn(II) ions showed no significant decrease and only 10% loss of emission intensity after three hours excitation (Fig. 4). Besides, we used IR780, a commonly-used commercial mitochondrial dye, which lost 8% fluorescence intensity under the same test conditions, which means this probe can be

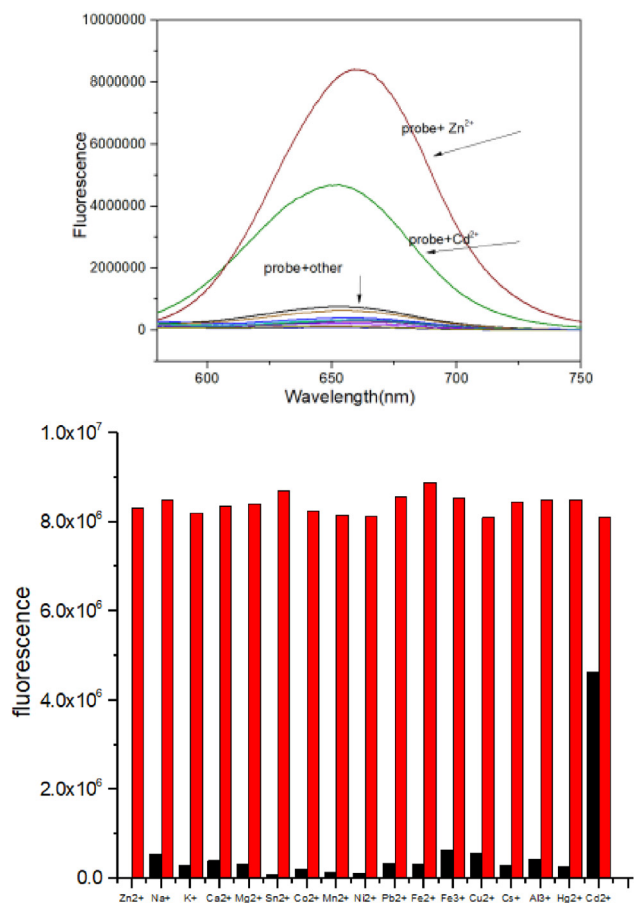


Fig. 6. Fluorescence spectral changes of 20 μM probe toward other metal ions; the red bars represent the emission intensity that occurs upon the subsequent addition of other metal ions to the probe NR-Zn with Zn(II) ions solution: Na^+ , K^+ , Ca^{2+} , Mg^{2+} , Sn^{2+} , Co^{2+} , Mn^{2+} , Ni^{2+} , Pb^{2+} , Fe^{2+} , Fe^{3+} , Cu^{2+} , Cs^+ , Al^{3+} , Hg^{2+} , Cd^{2+} , (in ethanol /pH 7.4 HEPES buffer = 3/7) (in ethanol /pH 7.4 HEPES buffer = 3/7, 0.9 mL/2.7 mL). (For interpretation of the references to color in this figure legend, the reader is referred to the web version of this article.)

used with good photostability (Fig. 8 and Fig. S13).

4. Cell imaging and cytotoxicity of probe NR-Zn

4.1. Cytotoxicity of probe NR-Zn

We use MTS method to assess the cytotoxicity of probe NR-Zn with HeLa cells. It shows that there is not any obvious impact on cell viability by incubation of the HeLa cells with 2 μM , 5 μM , 10 μM probes over 24 h, respectively. The cell still remained 85% viability even at the highest 10 μM concentration, the slight cytotoxicity indicated that the probe has good bio-compatibility and can be used as a good living cell staining dye (Fig. 9).

4.2. Cell imaging of probe NR-Zn

An evaluation of the ability to utilize the probe NR-Zn to detect Zn(II) ions in living cells was investigated by incubating HeLa cells with 0 μM , 2 μM , 5 μM Zn(II) ions; respectively. As shown in Fig. 10, no obvious fluorescence of cell imaging was addition of 2 μM Zn(II) ions to the probe NR-Zn pre-treated cells with 5 μM Zn(II) ion, an obvious fluorescence emission from probe was observed, indicating probe is membrane permeable and can sensitively detect the intracellular Zn(II) ion in bio-system. The fluorescence intensity of HeLa cells is maximum

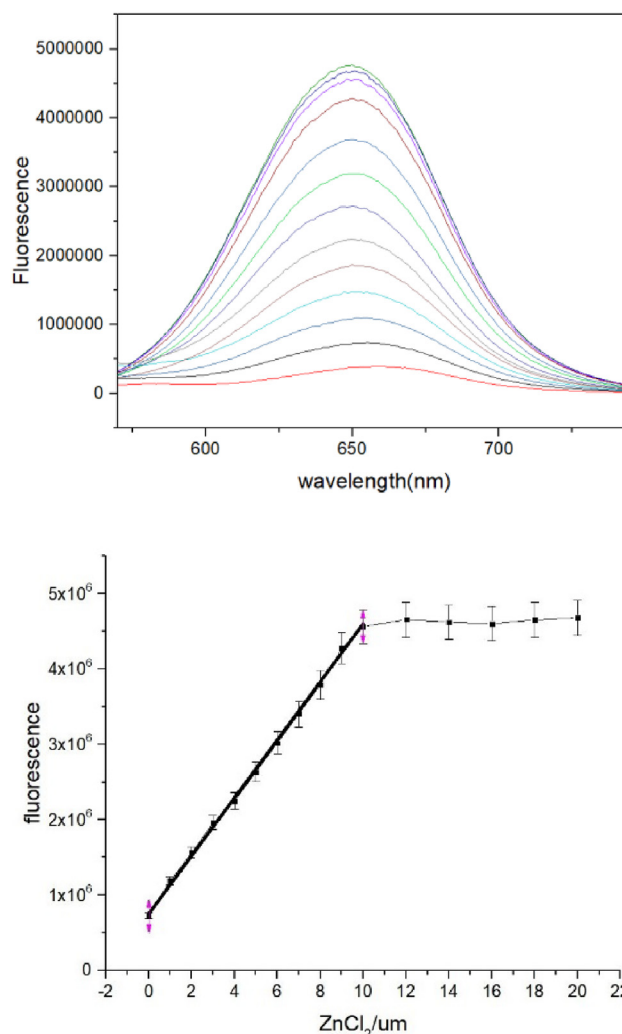


Fig. 7. Fluorescence spectra of 10.0 μM probe NR-Zn with ZnCl_2 from 0 μM to 20 μM (in ethanol/pH 7.4 HEPES buffer = 3/7, 0.9 mL/3.1 mL) and the corresponding Zn^{2+} titration profile of the emission at 660 nm.

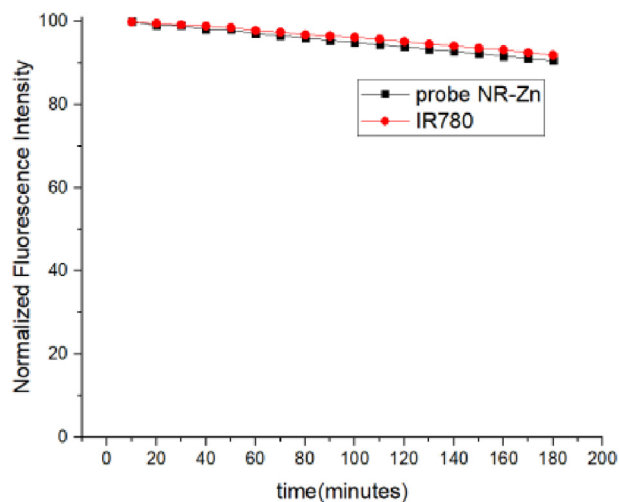


Fig. 8. Photostability of the probe NR-Zn and IR-780.

when 5 μM Zn(II) ions added into the probe NR-Zn pre-treated cells, which is the same to that of probe NR-Zn in solution. All of these results show that this probe can be applied to detect intracellular Zn(II) ions

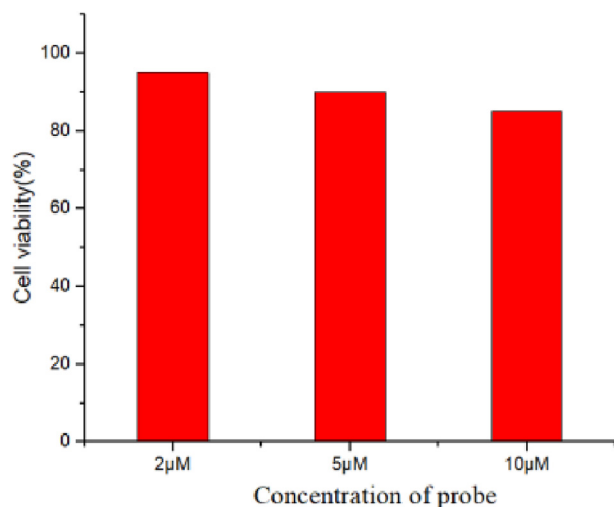


Fig. 9. Cytotoxicity experiments of probe conducted by MTS assay.

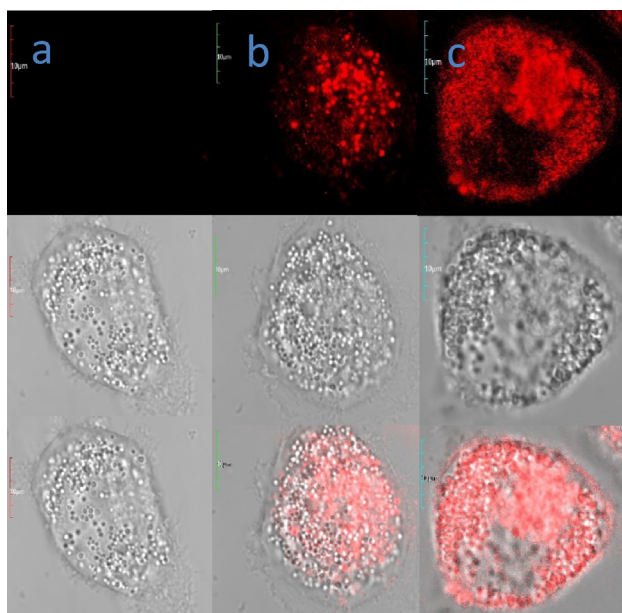


Fig. 10. Fluorescence images of fluorescent probe (5 μM) with different concentrations of Zn(II) ions (a: 0 μM, b: 2 μM, c: 5 μM) in HeLa cells. λ_{ex} : 559 nm.

concentration in HeLa cells.

Next, we investigated intracellular Zn(II) concentration changes in living cells by using our probe. As shown in Fig. 11, HeLa cells were first treated with 2,2'-dithiodipyridine (DTDP) for one hour, which has been reported to release Zn(II) ions from intracellular metallo proteins in HeLa cell [42]. Upon addition of probe to the cells, it can be found there was a significant increase in the fluorescence intensity of HeLa cells by the release of Zn(II) ions. These results unambiguously demonstrated that this fluorescent probe can be effectively used to detect Zn(II) ions changes in living cells (Fig. 11).

5. Conclusions

In conclusion, we reported a new fluorescent probe with high selectivity and sensitivity toward Zn(II) ions based on a dicyanoisophorone fluorophore. This probe can strongly bind Zn(II) ions to effectively trigger the fluorescence by ICT effect. This fluorescent probe offers a new method to track Zn(II) ions in living cells.

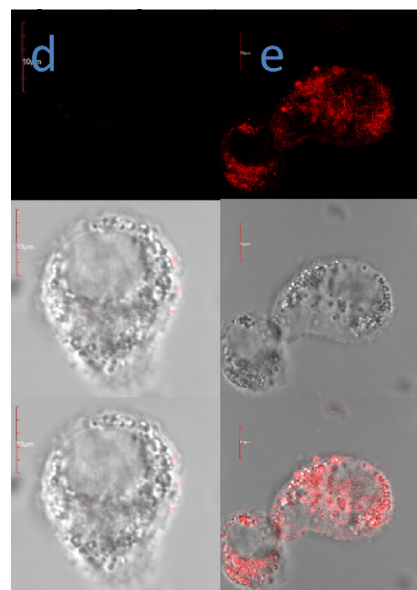


Fig. 11. d: Fluorescence images of HeLa cells incubated without DTDP (5 μM) and then detected by probe (10 μM). e: Fluorescence images of HeLa cells incubated with DTDP (5 μM) for 1 h and then detected by probe (10 μM). λ_{ex} : 559 nm.

Author contributions

The manuscript was written through the contributions of all authors.

Declaration of Competing Interest

The authors declare that they have no known competing financial interests or personal relationships that could have appeared to influence the work reported in this paper.

Appendix A. Supplementary data

Supplementary data to this article can be found online at <https://doi.org/10.1016/j.ica.2020.119640>.

References

- [1] J.M. Berg, H.A. Godwin, *Annu. Rev. Biophys. Biomol. Struct.* 26 (1997) 357–371.
- [2] H. Brismar, B. Ulfhake, *Nat. Biotechnol.* 15 (1997) 373–377.
- [3] L.M.T. Canzoniero, D.M. Turetsky, D.W. Choi, *J. Neurosci.* 19 (1999).
- [4] A.I. Bush, *Curr. Opin. Chem. Biol.* 4 (2000) 184–191.
- [5] G.K. Andrews, *Biometals* 14 (2001) 223–237.
- [6] Y. Chen, Y. Irie, W.M. Keung, W. Maret, *Biochemistry* 41 (2002) 8360–8367.
- [7] A.I. Bush, R.E. Tanzi, *Proc. Natl. Acad. Sci. U. S. A.* 99 (2002) 7317–7319.
- [8] C. Andreini, L. Banci, I. Bertini, A. Rosato, *J. Proteome Res.* 5 (2006) 3173–3178.
- [9] A. Atkinson, D.R. Winge, *Chem. Rev.* 109 (2009) 4708–4721.
- [10] S.H. Hou, Z.G. Qu, K.L. Zhong, Y.J. Bian, L.J. Tang, *Tetrahedron Lett.* 57 (2016) 2616–2619.
- [11] S.Y. Lee, S.Y. Kim, J.A. Kim, C. Kim, *J. Lumin.* 179 (2016) 602–609.
- [12] M.T. Morgan, A.M. McCallum, C.J. Fahrni, *Chem. Sci.* 7 (2016) 1468–1473.
- [13] P.R. Sahoo, K. Prakash, S. Kumar, *Coord. Chem. Rev.* 357 (2018) 18–49.
- [14] D. Wu, L. Chen, W. Lee, G. Ko, J. Yin, J. Yoon, *Coord. Chem. Rev.* 354 (2018) 74–97.
- [15] J.D. Zhang, M.Y. She, J. Li, C.L. Wang, S. Wang, P. Liu, S.Y. Zhang, J.L. Li, *Sens. Actuators, B* 270 (2018) 362–370.
- [16] P. Gao, W. Pan, N. Li, B. Tang, *Chem. Sci.* 10 (2019) 6035–6071.
- [17] P. Zhao, Q. Xu, J. Tao, Z. Jin, Y. Pan, C. Yu, Z. Yu, *WIREs Nanomed. Nanobiotechnol.* 10 (2018) e1483.
- [18] S. Sun, Q. Guan, Y. Liu, B. Wei, Y. Yang, Z. Yu, *Chin. Chem. Lett.* 30 (2019) 1051–1054.
- [19] S.M. Hwang, D. Yun, H. Lee, M. Kim, M.H. Lim, K.T. Kim, C. Kim, *Dyes Pigm.* 165 (2019) 264–272.
- [20] E. Senkuytu, E.T. Ecik, *Spectrochim. Acta Part A Mol. Biomol. Spectrosc.* 198 (2018) 232–238.

- [21] S.J. Park, Y.J. Kim, J.S. Kang, I.Y. Kim, K.S. Choi, H.M. Kim, *Anal. Chem.* 90 (2018) 9465–9471.
- [22] Q.F. Li, J.T. Wang, S.Y. Wu, G.W. Ge, J.B. Huang, Z.L. Wang, P.P. Yang, J. Lin, *Sens. Actuators, B* 259 (2018) 484–491.
- [23] Y.C. Chen, W.J. Zhang, Z. Zhao, Y.J. Cai, J.Y. Gong, R.T.K. Kwok, J.W.Y. Lam, H.H.Y. Sung, I.D. Williams, B.Z. Tang, *Angew. Chem.-Int. Ed.* 57 (2018) 5011–5015.
- [24] X.H. Tian, Q. Zhang, M.Z. Zhang, K. Uvdal, Q. Wang, J.Y. Chen, W. Du, B. Huang, J.Y. Wu, Y.P. Tian, *Chem. Sci.* 8 (2017) 142–149.
- [25] R.R. Nawimanage, B. Prasai, S.U. Hettiarachchi, R.L. McCarley, *Anal. Chem.* 89 (2017) 6886–6892.
- [26] Z. Xu, L. Xu, *Chem. Commun.* 52 (2016) 1094–1119.
- [27] H.J. Lee, C.W. Cho, H. Seo, S. Singha, Y.W. Jun, K.H. Lee, Y. Jung, K.T. Kim, S. Park, S.C. Bae, K.H. Ahn, *Chem. Commun.* 52 (2016) 124–127.
- [28] G.B. Zhang, Y.F. Zhao, B. Peng, Z. Li, C.C. Xu, Y. Liu, C.W. Zhang, N.H. Voelcker, L. Li, W. Huang, *J. Mater. Chem. B* 7 (2019) 2252–2260.
- [29] Z.Y. Chen, X.L. Mu, Z. Han, S.P. Yang, C.L. Zhang, Z.J. Guo, Y. Bai, W.J. He, *J. Am. Chem. Soc.* 141 (2019) 17973–17977.
- [30] X.D. Yang, Q. Jiang, P.F. Shi, *Prog. Chem.* 30 (2018) 1172–1185.
- [31] J. Yang, S.D. Zhai, H. Qin, H. Yan, D. Xing, X.L. Hu, *Biomaterials* 176 (2018) 1–12.
- [32] J. Xu, Z.K. Wang, C.Y. Liu, Z.H. Xu, B.C. Zhu, N. Wang, K. Wang, J.T. Wang, *Anal. Sci.* 34 (2018) 453–457.
- [33] Y.T. Xie, W.J. Cheng, B. Jin, C.G. Liang, Y.B. Ding, W.H. Zhang, *Analyst* 143 (2018) 5583–5588.
- [34] X.Y. Wen, Q. Wang, Z.F. Fan, *Anal. Chim. Acta* 1013 (2018) 79–86.
- [35] S. Zhang, R. Adhikari, M. Fang, N. Dorh, C. Li, M. Jaishi, J. Zhang, A. Tiwari, R. Pati, F.-T. Luo, H. Liu, *ACS Sensors* 1 (2016) 1408–1415.
- [36] W. Li, Z. Liu, B. Fang, M. Jin, Y. Tian, *Biosens. Bioelectron.* 148 (2020) 111666.
- [37] M. Fang, S. Xia, J. Bi, T.P. Wigstrom, L. Valenzano, J. Wang, M. Tanasova, R.L. Luck, H. Liu, *Molecules* 24 (2019) 1592.
- [38] J. Li, F. Huo, Z. Wen, C. Yin, *Spectrochim. Acta Part A Mol. Biomol. Spectrosc.* 221 (2019) 117156.
- [39] H.T. Ngo, X. Liu, K.A. Jolliffe, *Chem. Soc. Rev.* 41 (2012) 4928–4965.
- [40] G. Niu, P. Zhang, W. Liu, M. Wang, H. Zhang, J. Wu, L. Zhang, P. Wang, *Anal. Chem.* 89 (2017) 1922–1929.
- [41] D. Magde, R. Wong, P.G. Seybold, *75 (2002) 327–334.*
- [42] E. Aizenman, A.K. Stout, K.A. Hartnett, K.E. Dineley, B. McLaughlin, I.J. Reynolds, *J. Neurochem.* 75 (2000) 1878–1888.